Investigation of Thermal Expansion Effects on Si-Based MEMS Structures

Kirsten L. Brookshire, Ramin Rafiei, Mariusz Martyniuk, *Member, IEEE*, K. K. M. B. D. Silva, *Member, IEEE*, Lorenzo Faraone, *Fellow, IEEE*, and Yinong Liu

***Abstract*— This paper presents a study of the effects of stress and thermal expansion of inductively coupled plasma enhanced chemical vapor deposited (ICPCVD) amorphous Si thin films on low-temperature microelectromechanical systems test structures. Experimental data were used in conjunction with finite-element modeling (FEM) to predict deformation in simple microstructures across a wide temperature range from 85 to 300 K. Temperature dependence of residual stress and the coefficient of thermal expansion (CTE) of ICPCVD Si thin films was investigated by characterizing the curvature of bilayer thin-film samples through the use of optical profilometry at low temperature. Extracted parameters were used in an FEM package to confirm the experimental results by correlating with observed deformation of fabricated test structures. It is demonstrated that the experimentally determined CTE enables accurate modeling of the mechanical behavior of thin-film microstructures across a wide range of temperatures. [2015-0175]**

***Index Terms*— Bi-layer thin films, coefficient of thermal expansion (CTE), cryogenic, finite element modeling, inductively coupled plasma enhanced chemical vapor deposited (ICPCVD) Si, low-temperature, microelectromechanical systems (MEMS), stress, thin films.**

I. Introduction

ACCURATELY predicting the behavior of microelectromechanical systems (MEMS) is necessary for devices that function over a wide range of temperatures, thus enabling prudent design engineering prior to fabrication. This is of particular relevance for applications in which optical MEMS are combined with infrared sensing devices, which are typically cooled to cryogenic temperatures. Control of the internal stresses in thin films has long been critical for realization of reliable and stable MEMS devices [1], with Si-based materials being the most commonly used material in MEMS.

The stress observed at room temperature in inductively coupled plasma enhanced chemical vapour deposition (ICPCVD) silicon-based thin films has been reported previously [2]–[5]. Stress in multi-layer structures can result in catastrophic device failure as well as rendering the device unusable due to mechanical stiffening or distortion. Stresses in such structures can result from many factors: lattice mismatch between deposited layers, lattice mismatch between the substrate and deposited layers, different coefficient of thermal expansion (CTE) in materials, and variable thermal history inherent in ICPCVD processing [6].

Understanding the mechanisms that contribute to the observed stress states, and developing ways to mitigate them, is critical in MEMS design and application. Huang *et al.* studied the effects of residual stresses in ICPCVD silicon nitride cantilever and fixed-fixed beam structures [2]. Using finite element modeling (FEM) they identified a symmetric out-of-plane, or vertical, stress gradient of 275 MPa/μm ranging from 55 MPa compressive to 55 MPa tensile stress in cantilever beams of 0.4 μm in thickness. Many studies have reported on the intrinsic stress and residual strain in thin films. However, as noted by Huang *et al.*, little has been reported on stress gradients through the thickness of the film, which can impact distortion in ways that may obscure results from traditional residual stress measurement techniques such as fixed-fixed beam buckling and Guckle ring deformation.

One method for the evaluation of residual stress is through thin-film induced substrate bending, which provides a means for determining even relatively low levels of residual stress, on the order of tens of MPa, in a deposited film. This method of calculating stress has been used since 1909 when Stoney reported on the tension in electrolytically deposited metallic films [7]. Retajczyk *et al.* used this method in their study on the temperature dependence of elastic stiffness, CTE, and intrinsic and thermal stresses of deposited silicides and silicon nitrides [4]. This technique continues to be used to characterize film-on-substrate or bi-layer structures [8]–[10].

In devices that must operate over large temperature ranges, the deformation effects observed due to residual stresses are often compounded due to a mismatch in CTE between the substrate and the device layers [11]–[14]. One such example, addressed in [1], [15], and [16], is that of SiN_x-based MEMS which are processed at above 100 °C and operated at cryogenic temperatures. For silicon, Young's modulus (E) and Poisson's ratio (υ) vary little with temperature, although it has been observed that thin-film to substrate CTE mismatch induces stress upon cooling [17]. As discussed earlier, the presence of stress in a MEMS structure can result in undesired distortion or complete device failure. To design structures that are minimally affected by CTE mismatch, FEM can be used,

Manuscript received June 23, 2015; revised January 5, 2016; accepted March 11, 2016. Date of publication April 21, 2016; date of current version May 30, 2016. This work was supported by the Australian Research Council under Grant LP120100097 and Grant LP120200674. Subject Editor J. Brugger.

K. L. Brookshire is with the University of Western Australia, Perth, WA 6008, Australia (e-mail: kirsten.brookshire@research.uwa.edu.au).

R. Rafiei was with the Microelectronics Research Group, University of Western Australia, Perth, WA 6008, Australia. He is now with Ocular Robotics, Kingsgrove, NSW 2208, Australia (e-mail: ramin@ocularrobotics.com).

M. Martyniuk, K. K. M. B. D. Silva, L. Faraone, and Y. Liu are with the Microelectronics Research Group, University of Western Australia, Perth, WA 6008, Australia (e-mail: mariusz.martyniuk@uwa.edu.au; dilusha.silva@uwa.edu.au; laurie.faraone@uwa.edu.au; yinong.liu@uwa.edu.au).

Color versions of one or more of the figures in this paper are available online at http://ieeexplore.ieee.org.

Digital Object Identifier 10.1109/JMEMS.2016.2548485

requiring that the CTE of the material must first be known.

In this paper, the thin-film induced substrate bending effect is utilized to evaluate the change in stress with temperature of an ICPCVD Si thin film. The change in stress with temperature enables the determination of the CTE of the deposited material, which is then used in a FEM model of simple MEMS structures to evaluate against the observed experimental deformation of fabricated devices.

II. Formulation for the Determination of Thin film CTE

For FEM of MEMS devices operating across a wide range of temperatures, the temperature dependence of material and mechanical properties must be known. When the CTE, $\alpha_f(T)$, is assumed to be constant with temperature, FEM predictions of structure deformations as a function of temperature are highly inaccurate since CTE has a very strong impact on mechanical behavior from the induced internal stress in a thin-film substrate assembly due to CTE mismatch. Such in-plane stresses in the film and the substrate causes structural distortion, which provides an opportunity to determine the CTE values of the film and the substrate by characterizing the shape changes of a film-on-substrate bi-layer structure. Based on this concept, this section formulates $\alpha_f(T)$ determination of thin films on a substrate of known CTE, by measuring curvature change as a function of temperature.

When stress is present in a thin film deposited on a substrate, the assembly bends. The relationship between the stress in the film, σ_f, and the curvature, c, of this bilayer structure is described by the Stoney equation [7]:

$$\sigma_f = \frac{M_s d_s^2}{6Rd_f} = \frac{M_s d_s^2 c}{6d_f} \tag{1}$$

where M_s is the biaxial modulus of the substrate, d_s is the substrate thickness, d_f is the deposited film thickness, R is the radius of curvature, and curvature is simply defined as $c = 1/R$. If a bilayer structure is then cooled, the mismatch between the CTE of the two materials will induce additional stress and change the curvature of the sample [4], [16], [18]–[20], as described by [4]

$$\frac{d\sigma}{dT} = -M_f\left(\alpha_s - \alpha_f\right), \tag{2}$$

where M_f is the biaxial modulus of the deposited film, and α_f and α_s are the CTEs of the film and the substrate, respectively.

By knowing the CTE of the substrate and measuring the curvature change (thereby determining the stress change) with temperature, the CTE of the thin film can be determined using (2). However, this equation still contains two unknown parameters, M_f and α_f. Therefore, a second independent condition needs to be established. For this we deposit the same film on two different substrates, and (2) holds true for the following two simultaneous equations:

$$\frac{d\sigma_1}{dT} = -M_f\left(\alpha_{S1} - \alpha_f\right) \tag{3}$$

$$\frac{d\sigma_2}{dT} = -M_f\left(\alpha_{S2} - \alpha_f\right) \tag{4}$$

TABLE I
Deposition Conditions for ICPCVD a-Si

Gas Chemistry SiH_4/He (sccm)	Pressure (Pa)	Power (Watts)	Temperature (°C)
5/95	4	26	300

where the subscripts 1 and 2 refer to substrates 1 and 2, respectively.

By combining (3) and (4), an equation for the CTE of the film, α_f, can be derived:

$$\alpha_f = \frac{\alpha_{S2}\frac{d\sigma_1}{dT} - \alpha_{S1}\frac{d\sigma_2}{dT}}{\frac{d\sigma_1}{dT} - \frac{d\sigma_2}{dT}} \tag{5}$$

which requires the experimental determination of stress versus temperature for the film deposited on two different substrates, giving $d\sigma_1/dT$ and $d\sigma_2/dT$. It is assumed that (1) the choice of substrate does not result in any epitaxy in the film, (2) the substrate-film compositions have biaxial symmetry, and (3) the film thickness is much less than the substrate. It is also require that the sample have L > 5w, so transvers bending of the sample is not restricted [21].

III. Experimental Determination of Thin Film CTE

This section determines the CTE of a deposited film using film-induced substrate bending, which provides a simple method for the determination of CTE.

A. ICPCVD Si Film Deposition

CTE is determined by measuring the curvature of film-substrate bilayer samples. Two different substrates were used in this study 90 μm thick Si(100) and 110 μm thick Ge(100). The wafer substrates were cut to approximately 2 mm × 15 mm in dimension with the length aligned to the ⟨110⟩ crystallographic direction. Amorphous Si thin films were deposited onto the substrates using a Sentech SI 500D ICPCVD system using the deposition conditions summarized in Table I, with a resulting thin film thickness of 1 μm.

B. Experimental Setup for Low Temperature Optical Profilometry

Curvature of film-on-substrate samples was measured using a Zygo NewView 6K optical profilometer. Fig. 1 shows the cryostat used for the low temperature curvature. measurements, with the sheath on and a cut-out to reveal the Si diode, heater, and liquid nitrogen channel. Temperature was controlled via a PID control loop between the Si diode and the heater. A thermocouple was placed at the position where the sample is anchored to the cold finger (position "TC1" in Fig. 1) to monitor the at-sample temperature. In preliminary testing an additional thermocouple was placed at position "TC2" to evaluate the temperature difference between sample anchor point (TC1) and the sample end (TC2). The system was verified against a previously measured sample and no thermal gradient along the length of the sample was observed [22].

To conduct the measurement, a sample strip was mounted to the cryostat cold finger as shown in Fig. 1 (inset) using silver

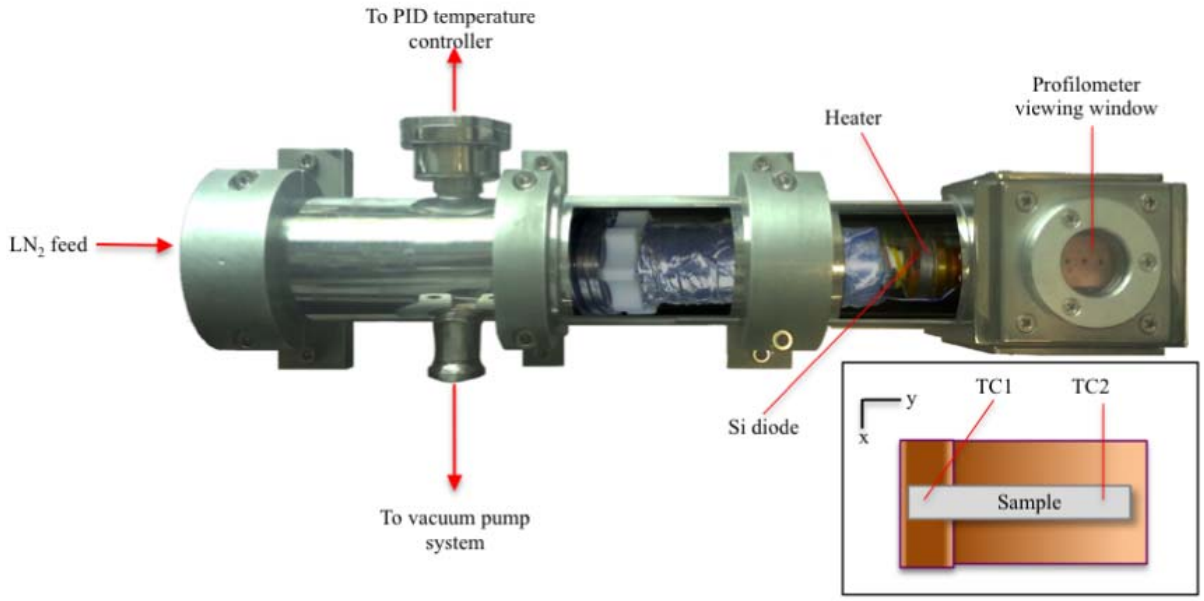

Fig. 1. Experimental setup for the measurement of curvature at low temperatures. The sample is placed at the end of the cold finger as shown in the inset and a single thermocouple is placed at position TC1.

TABLE II
RELEVANT MATERIAL PROPERTIES OF SUBSTRATES

Material	M <110>	CTE Equation	Source
Ge(100)	138 GPa	$\alpha = 2.4583\text{x}10^{-6} + (-1.58\text{x}10^{-7})T + (3.18\text{x}10^{-9})T^2 + (-2.17\text{x}10^{-11})T^3 + (6.43\text{x}10^{-14})T^4 + (-7.04\text{x}10^{-17})T^5$	[23, 24]
Si(100)	180 GPa	$\alpha = 1.88\text{x}10^{-6} + (-7.45\text{x}10^{-8})T + (7.45\text{x}10^{-10})T^2 + (-2.51\text{x}10^{-12})T^3 + (2.95\text{x}10^{-15})T^4$	[21, 25]
a-Si	130 GPa	$\alpha = -3.231\text{x}10^{-6} + (7.201\text{x}10^{-8})T + (-6.29\text{x}10^{-10})T^2 + (3.66\text{x}10^{-12})T^3 + (-1.12\text{x}10^{-14})T^4 + (1.31\text{x}10^{-17})T^5$	[26] and this work

epoxy. To maintain a uniform temperature across the sample, a copper thermal sheath with viewing holes was placed over the mounted sample, which is visible in the viewing window in Fig. 1. To allow the curvature of the sample to be imaged using the profilometer, the cryostat was fitted with a 3 mm thick BK7 window, which required the use of an objective lens with dispersion compensation for the optical profilometer. Prior to each measurement, a base pressure of 10^{-6} Torr was achieved for the cryostat.

C. Curvature Measurement

Curvature of the substrate wafer was measured prior to film deposition. The primary axes of the samples were aligned along the ⟨110⟩ directions of the substrate wafers, with the long axis labeled y and short axis labeled x. Curvature data was taken at different temperatures from room temperature (300 K) down to 85 K. At each temperature, the sets of curvature data were recorded, with stress being calculated from the curvature values using (1), and an average stress at each temperature was thus determined. A polynomial function was used as a least-squares fit to the stress versus temperature data, and the resulting change in stress with temperature $d\sigma/dT$, was used to determine the CTE of the film, $\alpha_f(T)$, using (5). To allow the use of (5) to determine film CTE from the measured $d\sigma/dT$ data, some material properties of the Si(100) and Ge(100) substrates are needed, as listed in Table II.

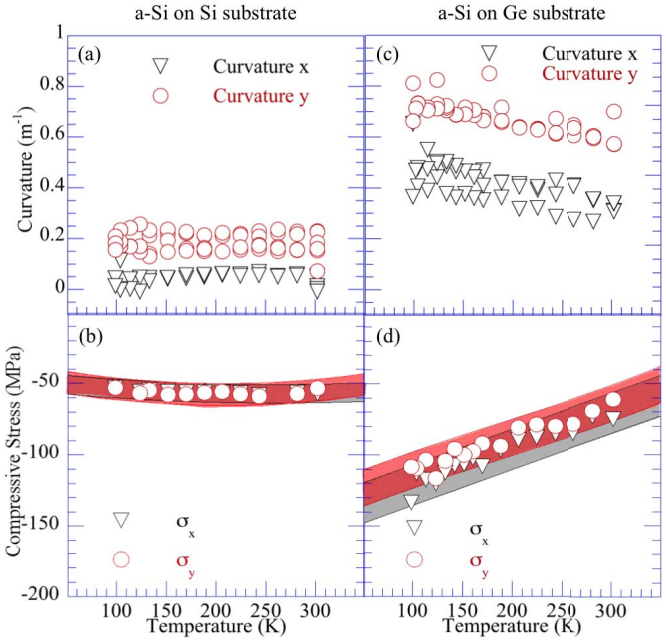

Fig. 2. Effect of temperature on curvature of PECVD Si on Ge(100) and Si(100) substrates. (a) and (b) correspond to ICPCVD a-Si deposited on a Si substrate. Fig. (c) and (d) correspond to ICPCVD a-Si deposited on a Ge substrate.

IV. DETERMINATION OF CTE OF ICPCVD Si THIN FILMS

Fig. 2 shows the effect of temperature on the measured curvature and the corresponding change in stress with temperature of the ICPCVD Si thin films. Figs. 2 (a) and (b) represent

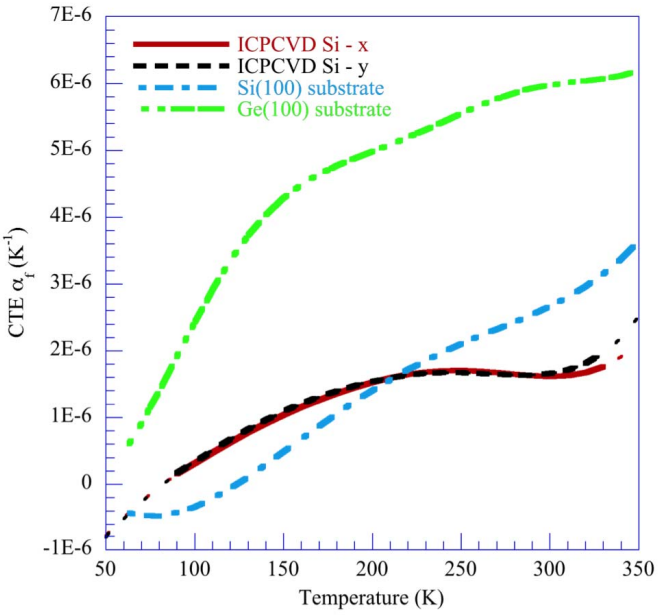

Fig. 3. Temperature dependence of the CTE of ICPCVD Si thin films, in comparison with those of Si (100) and Ge(100) wafers [21], [23], [25]. The CTE for ICPCVD Si is observed to cross the CTE of the Si substrate at 210 K.

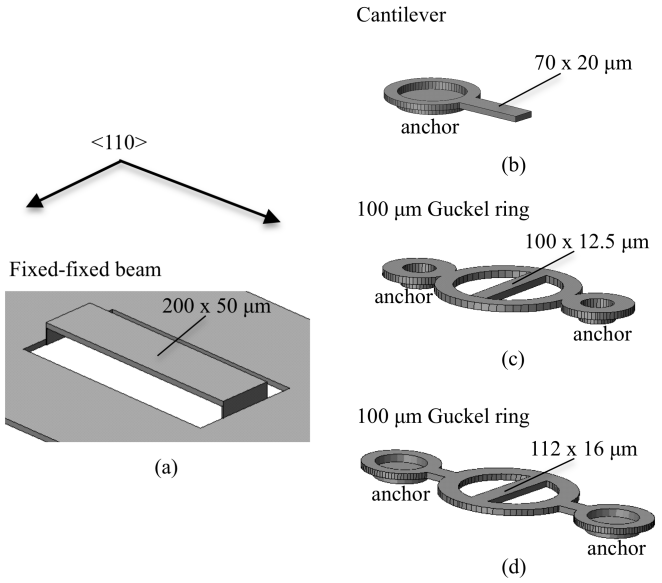

Fig. 4. Test structures used to evaluate the effect of CTE mismatch in experiments and in simulations: (a) fixed-fixed beam, (b) cantilever beam, (c) and (d) Guckel ring structures. The Si film is 1 um thick, and the heights in the drawings have been exaggerated 5x for ease of viewing.

Si deposited on the Si(100) substrate and Figs. 2 (c) and (d) represent Si deposited on Ge(100) substrates. The separation of curvature in x and y directions noted in Figs. 2 (a) and (c) results from the substrates having slightly different curvatures in the two directions prior to deposition. This is accounted for in the calculation of stress, and subsequent plots of stress data over lay in the x and y directions.

Figs. 2 (b) and (d) represent the change in stress with change in temperature for the Si/Si(100) and Si/Ge(100) samples, respectively. The data points are the average of four measurements taken at each temperature with two standard deviations in the data indicated by the error bands (red band corresponding to the error in the y-direction stress measurement and the grey band corresponding to the error in the x-direction stress measurement). Error propagation analysis from known sources of error provides a lower value than the two standard deviation values plotted in Fig. 2, the larger value was chosen for error reporting.

Within the temperature range of the measurement, ICPCVD Si on Ge(100) substrates demonstrate a positive correlation between thin film stress and temperature. Referring to (1) and (2), we see that a positive correlation between stress and temperature is indicative of the deposited film having a CTE lower than that of the substrate, whereas a negative correlation indicates that the film has a higher α value than that of the substrate. This is consistent with the expected values for ICPCVD Si [9], [10], [27].

A polynomial approximation of the temperature dependence of stress, $\sigma = f(T)$, was best fitted using the least-squares method for the data shown in Fig. 2. The polynomials, $d\sigma_1/dT$ for the Si/Ge(100) sample and $d\sigma_2/dT$ for the Si/Si(100), as shown in Fig. 2, were then used in (5) to calculate the temperature dependence of CTE, $\alpha_f\,(T)$, for the ICPCVD Si films on two different substrates. Fig. 3 shows the $\alpha_f\,(T)$ for the ICPCVD Si films. Also plotted in Fig. 3 are the CTEs of Si(100) and Ge(100) wafers in the ⟨110⟩ directions, as expressed in Table II, for comparison. The polynomial equation that best describes the CTE for ICPVD a-Si is also reported in Table II. It is noted that the deposited a-Si thin film has a CTE as a function of temperature that is very similar to that of the Si substrate.

The most notable feature of the curves shown in Fig. 3, is that the CTE of the deposited a-Si crosses the value for the substrate CTE at approximately 210 K. This is a significant finding as a crossing of CTE would be evident by the deformation behavior observed in a microstructure that is affected by CTE mismatch. As the temperature is reduced the apparent stress in the deposited material would become increasingly compressive down to 210 K. In contrast, below this temperature the thin film stress would become increasingly tensile.

Using the experimentally determined CTE of a-Si and Equation 2, the elastic modulus, M_f, for the deposited material can be determined. Using the data in Fig. 2b and 2d for $d\sigma/dT$, $M_f = 120$ GPa $\pm$ 20 GPa across the range of 70 K to 300 K. This value is in agreement with previously reported values of elastic modulus for ICPCVD a-Si [26].

V. Effect of CTE Mismatch on Si/Substrate Test Structures

Cooling-induced structure deformation of a number of MEMS test structures was characterized by means of both experimentation and finite element modeling (FEM) using the CTE data determined above. Fig. 4 shows the designs of the test structures, including cantilever beams (Fig. 4 (b)), fixed-fixed beams (Fig. 4 (a)) and Guckel rings [28] (Figs. 4 (c) and (d)). The a-Si films were 1 um thick with microstructures alligned along the ⟨110⟩ directions of the

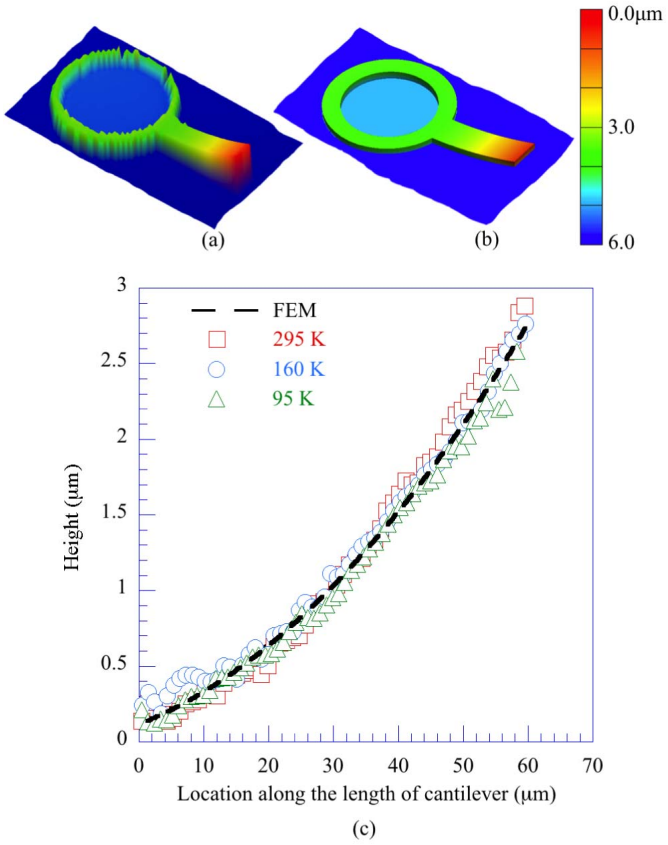

Fig. 5. Bending of an a-Si cantilever beam caused by an out-of-plane thin film stress gradient of 160 MPa/μm. (a) Optical profilometry image of the fabricated cantilever; (b) FEM modelling of the cantilever; (c) comparison of the height displacement profiles of the cantilever along the length between the experimental results and FEM.

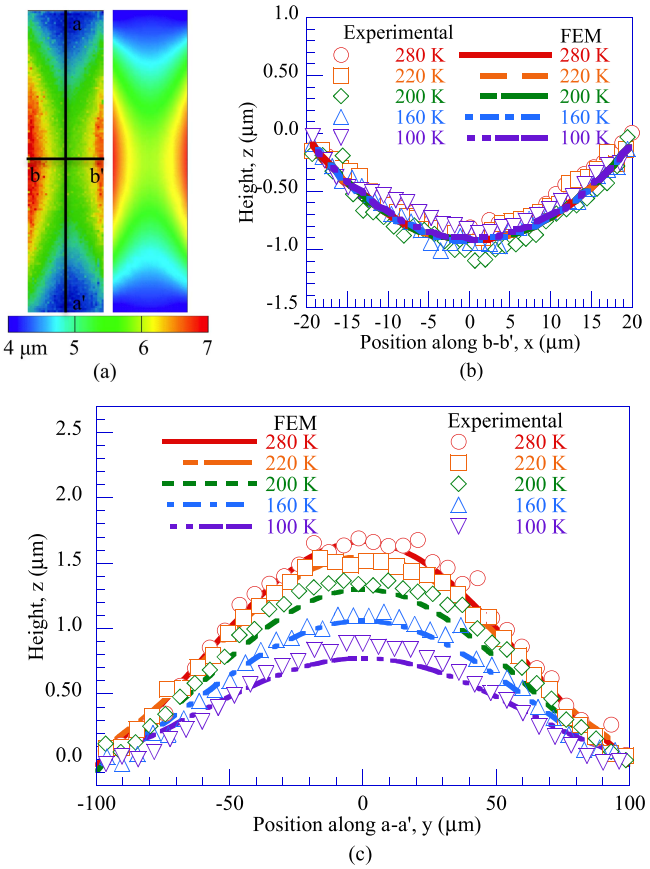

Fig. 6. Effect of cooling on profile distortion of a fixed-fixed beam. (a) Measured optical profile (left) and FEM model (right) images of the fixed-fixed beam at 160 K. (b) Beam profile across the width, b – b', at different temperatures. (c) Beam profile along the length, a – a', at different temperatures.

Si substrate. A sacrificial spacing layer of polyimide was used to create the space between the substrate and the free-standing MEMS structures, with anchor points being used to fix the structure to the substrate. The structures were released by dry etching the polyimide in an oxygen plasma in a barrel asher at 150 Watts for 15 minutes.

When depositing films via ICPCVD at elevated temperatures, an out-of-plane stress gradient often develops [2], that can be further enhanced during release steps when the deposited Si is exposed to an oxygen plasma. Such a stress gradient is independent of temperature, thus not affecting the CTE calculations above, but it is critical in accurately modeling device behavior. Stress gradients may also confound information obtained from Guckel rings and fixed-fixed beam test structures. The cantilever structures, which are only sensitive to vertical stress gradients, were used to evaluate the stress gradient through the film thickness, whereas the Guckel rings and fixed-fixed beams were used to evaluate stress changes with temperature due to CTE mismatch between the film and the substrate.

Fig. 5 shows the observed distortion of an a-Si cantilever beam, with Fig. 5 (a) indicating the optical profilometry data of a cantilever beam at room temperature (300 K). Using the stress strain equation, $\sigma = E\varepsilon$, with Young's modulus of 130 GPa for the ICPCVD a-Si [26] and strain in the cantilever determined from the curvature of the beam in Fig. 5 (a), the stress gradient through the thickness of the film is determined to be $d\sigma/dz = 160$ MPa/μm. Fig. 5 (b) is the result of FEM simulation of the profile of the cantilever, using a film modulus of 130 GPa, the experimentally determined film stress gradient of 160 MPa/μm, and parameters from Table II for the Si(100) substrate. It is noted that good agreement between the model and the experimental data is observed, confirming the value of calculated stress gradient.

Fig. 5 (c) plots the profile along the length of the cantilever as measured at three different temperatures. It is seen that the deflection in the cantilever did not change with temperature, indicating that the observed curvature is purely a feature of stress gradient within the deposited film and not a feature of CTE mismatch at the anchor.

The first structure used to evaluate thin film deformation due to CTE mismatch was the fixed-fixed beam shown in Fig. 4 (a). The beam was cooled in the system shown in Fig. 1, and optical profile data was taken at different temperatures ranging from 85 K to 300 K. Using the stress gradient (Fig. 5) and the experimentally determined CTE (Fig. 3) of the ICPCVD a-Si film, along with the film Young's modulus [26] and substrate parameters (Table II), the fixed-fixed beam was modeled to evaluate the effect of CTE mismatch on cooling-induced shape distortion.

Modelling results were compared to the experimental data, and Fig. 6 shows the change in beam shape with temperature. Fig. 6 (a) shows experimental optical profilometery data for the fixed-fixed beam and the FEM beam at 160 K. Fig. 6 (b) shows the profile of the beam along the center of the length direction (from a to a' as indicated in Fig. 6 (a)) at various temperatures, for both the experimental and FEM data. It is noted that at ambient temperature (300 K), the released beam shows a positive bowing upwards in the length direction. While upward bending in a beam with zero out-of-plane stress gradient would indicate a compressive film, FEM indicated that the previously determined out-of-plane stress gradient of 160 MPa/μm was sufficient to cause the beams to bend up in the observed manner. In fact, an average 80 MPa tensile stress was determined through FEM analysis of the fixed-fixed beam microstructures.

The results in Fig. 6 indicate that as the fixed-fixed beam sample is cooled, the beam begins to flatten. This implies that the film is becoming more tensile due to the film contracting more than the substrate, indicating a film CTE that is greater than that of the substrate. This experimental observation is consistent with the measured data presented in Fig. 3. Fig. 6 (b) shows the profile across the width of the beam, as measured from b to b' as indicated in Fig. 6 (a). The negative bowing across the beam width results from the film being relatively more compressive on the bottom and more tensile on the top due to the 160 MPa/μm out-of-plane gradient present in the films. Since the width is not constrained and free to deform, no large variation in profile with change in temperature due to differences in CTE is expected.

Experimentally, as the temperature changed, no corresponding change in curvature of the beam across its width was observed.

Fig. 7 shows two Guckle ring structures, which were also used to evaluate the CTE mismatch induced thin film deformation. The Guckle rings pictured in Figs. 7 (a) and (d) are designed such that the central beam bows or buckles when the film is under tensile stress, or remains flat when the deposited film is under compressive stress, with the amount of bowing indicating the magnitude of tensile stress in the film. Bowing will also be induced by any out-of-plane stress gradient in the film. Since two mechanisms for bowing are present, FEM was used to evaluate the room temperatures stress state.

The overall deformation in the structures indicated that the films were under an average tensile stress of 80 MPa at room temperature, in agreement with the value obtained from analysis of the fixed-fixed beam test structures. Fig. 7 (b) and (e) show the optical profilometry and FEM data for the cross beam of the 100 μm and 112 μm diameter Guckel ring structures at 180 K. Fig. 7 (c and f) plot the change in curvature of the central cross beam with change in temperature. Note that a rapid change in the direction of deformation is observed in the 100 μm Guckel ring at 200 K, whereas a more gradual change is observed in the larger 112 μm ring.

Referring back to Fig. 3, the plot of CTE for the deposited Si film, we see that the CTE of the deposited Si crosses the CTE of the silicon substrate at approximately 210 K. This crossing causes the deformation behavior of the deposited a-Si film to switch about this point. When cooling from 300 K to 210 K the radius of curvature of the cross beam in the Guckel ring will increase, indicating a reduction in tensile stress in the deposited film due to the fact that the film CTE is less than that of the substrate. For cooling below 210 K the radius of curvature reduces, indicating an increase in tensile stress in the

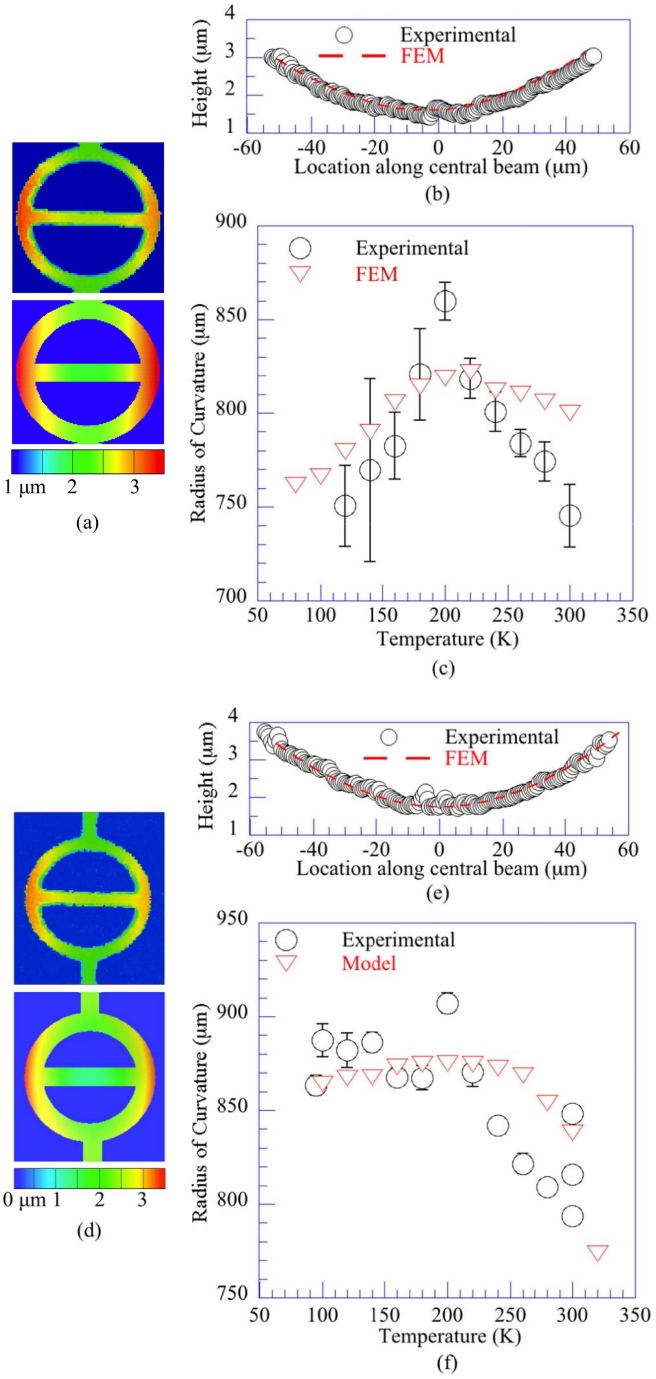

Fig. 7. Effect of cooling on cross-beam distortion of Guckel ring test structures. (a) and (d) Optical image (upper) and FEM model image (lower) of the 100 μm and 112 μm diameter Guckel rings, respectively. (b) and (e) Plots of the profile along the length of the central beam of the 100 μm and 112 μm cross-beams, respectively, comparing the experimental distortion to the FEM prediction at 160 K. (c) and (f) Plots of the change in radius of curvature with temperature of the central beam of the 110 μm and 112 μm cross-beams, respectively, comparing the experimental observation to the FEM predictions.

film due to the film CTE now being greater than the substrate. A similar behavior is observed in the larger 112 μm beam shown in Fig. 7 (f), where the radius of curvature increases as temperature is reduced to 210 K, and then remains relatively constant when cooled below this value. The FEM data shows good agreement with the experimental results.

VI. Summary and Conclusions

The CTE for ICPCVD Si has been determined using the two-substrate method. Above 210 K CTE for the deposited a-Si thin film is lower than the substrate, which leads to increases in compressive stress in the film as it is cooled. Below 210 K the CTE of the film became greater than the substrate, which leads to increases in tensile stress in the deposited film as it is cooled. The small difference in CTE between the Si substrate and the a-Si film had significant impact on the deformation of simple MEMS structures.

FEM of the Guckel rings, fixed-fixed beams, and cantilevers showed good agreement with the experimental observation from 85 K to 300 K. The cantilevers are a valuable tool for evaluating out-of-plane stress gradient present in deposited films.

The fixed-fixed beam showed a decrease of curvature upon cooling in accordance with the experimentally determined CTE for the a-Si. As predicted through FEM, the change in temperature between 300 K and 210 K did not increase the deformation profile of the beam. However, below 210 K the increase in tensile stress worked to flatten the beam.

The FEM model also predicted the deformation behavior of the two Guckel rings due to the CTE mismatch between deposited a-Si and the substrate. As the rings were cooled the radius of curvature of the central cross beam increased. This indicated a decrease in tensile stress, resulting from a film CTE being lower than the substrate. Below 210 K, the radius of curvature began to decrease, indicating an increase in tensile stress in the film, resulting from a film CTE being greater than that of the substrate.

The cryostat with the optical profilometer set-up makes possible the observation of low temperature deformation in bilayer films and simple MEMS structures. Utilizing this tool, the two-substrate method provides a simple means of accurately determining CTE from wafer bow. A precise CTE, enables the accurate modeling of thermally induced deformation of MEMS down to low temperatures. This capability allows for pre-fabrication predictive modeling of increasingly complex structures, giving an opportunity for short loop design steps aimed at reducing low temperature deformation of MEMS.

References

[1] M. Martyniuk, J. Antoszewski, C. A. Musca, J. M. Dell, and L. Faraone, "Stress in low-temperature plasma enhanced chemical vapour deposited silicon nitride thin films," *Smart Mater. Struct.*, vol. 15, no. 1, pp. S29–S38, 2006.

[2] H. Huang *et al.*, "Determination of mechanical properties of PECVD silicon nitride thin films for tunable MEMS Fabry–Pérot optical filters," *J. Micromech. Microeng.*, vol. 15, no. 3, pp. 608–614, 2005.

[3] H. Huang *et al.*, "Effect of deposition conditions on mechanical properties of low-temperature PECVD silicon nitride films," *Mater. Sci. Eng. A-Struct. Mater. Prop. Microstruct. Process.*, vols. 435–436, pp. 453–459, Nov. 2006.

[4] T. F. Retajczyk, Jr., and A. K. Sinha, "Elastic stiffness and thermal expansion coefficients of various refractory silicides and silicon nitride films," *Thin Solid Films*, vol. 70, no. 2, pp. 241–247, 1980.

[5] Y. Q. Fu, J. K. Luo, S. B. Milne, A. J. Flewitt, and W. I. Milne, "Residual stress in amorphous and nanocrystalline Si films prepared by PECVD with hydrogen dilution," *Mater. Sci. Eng. B-Solid State Mater. Adv. Technol.*, vols. 124–125, pp. 132–137, Dec. 2005.

[6] L. B. Freund and S. Suresh, *Thin Film Materials: Stress, Defect Formation and Surface Evolution*. Cambridge, U.K.: Cambridge Univ. Press, 2003.

[7] G. G. Stoney, "The tension of metallic films deposited by electrolysis," *Proc. R. Soc. London Ser. A, Contain. Papers Math. Phys. Character*, vol. 82, pp. 172–175, May 1909.

[8] R. E. Sah *et al.*, "Mechanical and electrical properties of plasma and thermal atomic layer deposited Al_2O_3 films on GaAs and Si," *J. Vac. Sci. Technol. A*, vol. 31, p. 041502, Jul./Aug. 2013.

[9] M. M. de Lima, Jr., R. G. Lacerda, J. Vilcarromero, and F. C. Marques, "Coefficient of thermal expansion and elastic modulus of thin films," *J. Appl. Phys.*, vol. 86, pp. 4936–4942, Nov. 1999.

[10] F. Jansen, M. A. Machonkin, N. Palmieri, and D. Kuhman, "Thermomechanical properties of amorphous silicon and nonstoichiometric silicon oxide films," *J. Appl. Phys.*, vol. 62, pp. 4732–4736, Dec. 1987.

[11] C. Patel, P. McCluskey, and D. Lemus, "Performance and reliability of Mems gyroscopes at high temperatures," in *Proc. 12th IEEE Intersoc. Conf. Thermal Thermomech. Phenomena Electron. Syst.*, Jun. 2010, pp. 1–5.

[12] N. Marsi, B. Y. Majlis, A. A. Hamzah, and F. Mohd-Yasin, "The mechanical and electrical effects of MEMS capacitive pressure sensor based 3C-SiC for extreme temperature," *J. Eng.*, vol. 2014, 2014, Art. no. 715167, doi: 10.1155/2014/715167.

[13] C. Brown, A. S. Morris, A. I. Kingon, and J. Krim, "Cryogenic performance of RF MEMS switch contacts," *J. Microelectromech. Syst.*, vol. 17, no. 6, pp. 1460–1467, Dec. 2008.

[14] S. S. Attar, S. Setoodeh, R. R. Mansour, and D. Gupta, "Low-temperature superconducting DC-contact RF MEMS switch for cryogenic reconfigurable RF front-ends," *IEEE Trans. Microw. Theory Techn.*, vol. 62, no. 7, pp. 1437–1447, Jul. 2014.

[15] M. Martyniuk, J. Antoszewski, C. A. Musca, J. M. Dell, and L. Faraone, "Stress response of low temperature PECVD silicon nitride thin films to cryogenic thermal cycling," in *Proc. Conf. Optoelectron. Microelectron. Mater. Devices*, 2004, pp. 381–384.

[16] M. Martyniuk, J. Antoszewski, C. A. Musca, J. M. Dell, and L. Faraone, "Environmental stability and cryogenic thermal cycling of low-temperature plasma-deposited silicon nitride thin films," *J. Appl. Phys.*, vol. 99, p. 053519, Mar. 2006.

[17] J.-H. Zhao, Y. Du, M. Morgen, and P. S. Ho, "Simultaneous measurement of Young's modulus, Poisson ratio, and coefficient of thermal expansion of thin films on substrates," *J. Appl. Phys.*, vol. 87, pp. 1575–1577, Feb. 2000.

[18] W. Fang and C.-Y. Lo, "On the thermal expansion coefficients of thin films," *Sens. Actuators A, Phys.*, vol. 84, pp. 310–314, Sep. 2000.

[19] W. Fang, H.-C. Tsai, and C.-Y. Lo, "Determining thermal expansion coefficients of thin films using micromachined cantilevers," *Sens. Actuators A, Phys.*, vol. 77, pp. 21–27, Sep. 1999.

[20] J.-H. Jou and L. Hsu, "Stress analysis of elastically anisotropic bilayer structures," *J. Appl. Phys.*, vol. 69, pp. 1384–1388, Feb. 1991.

[21] M. A. Hopcroft, W. D. Nix, and T. W. Kenny, "What is the Young's modulus of silicon?" *J. Microelectromech. Syst.*, vol. 19, no. 2, pp. 229–238, Apr. 2010.

[22] K. L. Brookshire *et al.*, "Cryogenic optical profilometry for the calculation of coefficient of thermal expansion in thin films," *Proc. SPIE*, vol. 8923, p. 89231V, Dec. 2013, doi: 10.1117/12.2033802.

[23] S. I. Novikova, "Thermal expansion of germanium at low temperatures," *Soviet Phys.-Solid State*, vol. 2, no. 1, pp. 37–38, 1960.

[24] J. J. Wortman and R. A. Evans, "Young's modulus, shear modulus, and Poisson's ratio in silicon and germanium," *J. Appl. Phys.*, vol. 36, no. 1, pp. 153–156, 1965.

[25] K. G. Lyon, G. L. Salinger, C. A. Swenson, and G. K. White, "Linear thermal expansion measurements on silicon from 6 to 340 K," *J. Appl. Phys.*, vol. 48, no. 3, pp. 865–868, 1977.

[26] K. L. Brookshire, M. Martyniuk, K. K. M. B. D. Silva, Y. Liu, and L. Faraone, "Long-term stability of ICPCVD a-Si under prolonged heat treatment," in *Proc. COMMAD*, Perth, WA, Australia, Dec. 2014, pp. 160–163.

[27] A. Witvrouw and F. Spaepen, "Viscosity and elastic constants of amorphous Si and Ge," *J. Appl. Phys.*, vol. 74, pp. 7154–7161, Dec. 1993.

[28] H. Guckel, D. Burns, C. Rutigliano, E. Lovell, and B. Choi, "Diagnostic microstructures for the measurement of intrinsic strain in thin films," *J. Micromech. Microeng.*, vol. 2, no. 2, p. 86, 1992.

Kirsten L. Brookshire received the B.A. degree in physics from Willamette University, Salem, OR, in 2009, and the M.S. degree in materials science from Oregon State University, Corvallis, OR, in 2011. She is currently pursuing the Ph.D. degree in mechanical and electrical engineering from the University of Western Australia. Her current research activities involve design, fabrication, and characterization of optical MEMS and materials characterization.

Ramin Rafiei received the Ph.D. degree in experimental nuclear physics from Australian National University. He is a recipient of the University Medal in Engineering and Physics.

Dr. Rafiei is a Director and an Academic Entrepreneur whose career spans the aerospace, automotive, nuclear, photonics, and robotics industries. He has a strong track record in new generation sensor development and a passion for bringing innovation to market.

Mariusz Martyniuk was born in Poland in 1976. He received the B.Sc. (Hons.) degree from the University of Toronto, ON, Canada; the M.A.Sc. degree from McMaster University, ON; and the Ph.D. degree from the University of Western Australia (UWA), Perth, Australia, in 2007.

He was with the industry sector as an Electronics Engineer before rejoining UWA, where he is currently a Research Professor with the Microelectronics Research Group and manages the Western Australian Node of the Australian National Fabrication Facility. His primary areas of interest encompass thin-film materials and thin-film mechanics, and their applications in microelectromechanical systems and optoelectronic devices.

Dr. Martyniuk's research contributions were recognized by the Inaugural Australian Museum Eureka Prize (the Oscars of Australian Science) for Outstanding Science in Support of Defence or National Security Award in 2008.

K. K. M. B. D. Silva was born in Sri Lanka in 1973. He received the Honours degrees in physics and electronic engineering from the University of Western Australia (UWA), and the Ph.D. degree in optical imaging technologies for biomedical applications in 2004.

He has worked both in industry and academia, and is currently a Research Professor and the Engineering Manager with the Microelectronics Research Group, UWA. Since returning to UWA in 2009, his research interests include optical MEMS sensors, optical spectroscopic sensors, and MEMS biosensors. He has attracted funding for his research from the agriculture and aerospace sectors, and the government, and is presently leading a number of MEMS related research efforts at MRG with strong commercial links to both the agricultural and aerospace sectors.

Lorenzo Faraone was born in Italy in 1951. He received the Ph.D. degree from the University of Western Australia (UWA), Perth, WA, Australia, in 1979.

He was a Research Scientist at Lehigh University, Bethlehem, PA, USA, from 1979 to 1980, where he was involved in studies on MOS devices. From 1980 to 1986, he was a member of the Technical Staff at RCA Laboratories, David Sarnoff Research Center, Princeton, NJ, USA, where he was involved in very large scale integration CMOS and non-volatile memory technologies, and space radiation effects in silicon-on-sapphire MOS integrated circuits. He joined the School of Electrical, Electronic, and Computer Engineering, UWA, in 1987, where he has been a Professor since 1998 and the Head of the Department/School from 1999 to 2003. Since joining UWA, his research interests have been in the areas of compound semiconductor materials and devices, and microelectromechanical systems (MEMS). He has supervised more than 30 Ph.D. student completions, and published more than 300 refereed technical papers in journals and conference proceedings.

Prof. Faraone received the RCA Laboratories Individual Outstanding Achievement Award in 1983 and 1986, and the John de Laeter Innovation Award in 1997. He is a member of the Order of Australia, and a fellow of the Australian Academy of Science and the Australian Academy of Technological Sciences and Engineering.

Yinong Liu was born in China in 1957. He received the Ph.D. degree in mechanical engineering from the University of Western Australia (UWA) in 1991.

He has been an Academician for the past 25 years, and is currently a Professor of Materials Engineering with UWA. His research interests include thin films for MEMS, shape memory alloys, magnetic materials, solid phase transformations, functional nanomaterials, and industrial corrosion. He also serves on the Editorial Boards of four international scholarly journals and international advisory committees of several conferences.